Iteratively Detected Twisted-Pair MIMO-OFDM Transmission with Far-End Crosstalk

Ahrens, Andreas; Lange, Christoph

Abstract— ***Crosstalk between neighbouring wire pairs in multi-pair copper cables has long been seen as an major source of disturbance that essentially limits the transmission quality and the throughput of such cables. However, van Ettens pioneering work has shown that multi-pair copper cables can be treated as MIMO (multiple input multiple output) channels and tremendous performance improvements are possible if appropriate signal processing is applied. For high-rate transmission, often the strong near-end crosstalk (NEXT) disturbance is avoided or suppressed and only the far-end crosstalk (FEXT) remains as crosstalk influence. Therefore in this contribution, the effects of FEXT in iteratively detected and SVD-assisted MIMO-OFDM transmission schemes are studied. Contrary to the cancellation of the crosstalk, which has achieved a level of maturity, the far-end crosstalk paths are viewed as additional transmission paths, which together with the wanted signal path convey the signal from the near to the far cable end. Extrinsic information transfer (EXIT) charts are used for analyzing and optimizing the convergence behaviour of the iterative demapping and decoding.***

Index Terms— ***Twisted-Pair Cable, OFDM, Multiple Input Multiple Output System, Singular Value Decomposition, Iterative Detection, EXIT Chart.***

1. Introduction

Crosstalk as an electromagnetic coupling between adjacent wire pairs has long been seen as one of the limiting disturbances in high-speed local cable networks [2]. Since van Ettens pioneering work in the mid 70's [3] it is well-known that if multi-pair copper cables are treated as MIMO (multiple input multiple output) channels tremendous performance improvements are possible. Therefore appropriate signal processing techniques such as singular value decomposition (SVD) known from wireless MIMO transmission systems have to applied. If multi-channel techniques treat several "traditional" channels as a whole and a "generalized" channel appears, inescapable improvements in the channel capacity can be expected as shown in [4]. Finally, from broadband radio transmission channels, it is well-known that MIMO techniques are able to overcome the limiting factor of multipath propagation known from single-carrier transmission schemes [5], [6]. Often short cables are used in high-speed data rate systems in fi ed access networks, e. g., if optical fibr transmission is used up to a street cabinet or a building and the last drop is bridged by copper cables. Since the near-end crosstalk (NEXT) is a very strong disturbance [2], several techniques have been developed in order to avoid or suppress NEXT [7]. Furthermore, in today's DSL transmission systems (digital subscriber line) often frequency duplex schemes are used. In these cases only the far-end crosstalk (FEXT) remains as a crosstalk influenc . Interestingly, investigations in [8] have shown that the FEXT impact is much stronger in short cables than in longer ones. As shown in [8], FEXT could be a real catalyst for the overall performance at high signal-to-noise ratio (SNR) in uncoded systems if appropriate signal processing is applied. However, coded systems are able to work in a much lower SNR region. Therefore, in this contribution the FEXT impact in an iteratively detected and SVD-assisted MIMO-OFDM transmission scheme is studied [9]. The proposed iterative decoder structures employ symbol-by-symbol soft-output

Manuscript received June 30, 2008, revised December 20, 2008. Parts of this paper are published in the conference record of the International Conference on Signal Processing and Multimedia Applications (SIGMAP), Porto (Portugal), July 26–29, 2008 [1]. Andreas Ahrens is with the Hochschule Wismar, University of Technology, Business and Design, Faculty of Engineering, Department of Electrical Engineering and Computer Science, Philipp-Müller-Straße, PO box 1210, 23952 Wismar, Germany, email: andreas.ahrens@hs-wismar.de. Christoph Lange is with T-Systems Enterprise Services GmbH, Goslarer Ufer 35, 10589 Berlin, Germany, email: christoph.lange@t-systems.com.

decoding based on the Bahl-Cocke-Jelinek-Raviv (BCJR) algorithm and are analyzed under the constraint of a fi ed data rate [10]. Transmitting a multicarrier modulated signal over each wire-pair within a multi-pair copper cable, the influ ence of the crosstalk can be modelled on each subcarrier independently. However, the cancellation of the crosstalk using transmit zero-forcing or Tomlinson-Harashima precoding has achieved a state of maturity. Therein the increase of the transmit power by using transmit zero-forcing can be avoided by using a non-linear modulo operation within the Tomlinson-Harashima precoding [11]–[13]. Finally, postprocessing such as zero-forcing suffers from an increased noise power. Therefore singular value decomposition based signal processing seems to be a real alternative, where neither the transmit power nor the noise power is increased.

The remainder of this paper is organized as follows: Section 2 introduces the cable characteristics and in section 3 the MIMO-OFDM system model is introduced and the performance metrics are given. The channel-encoded MIMO-OFDM system is introduced in section 4, while the associated performance results are presented and interpreted in Section 5. Section 6 provides our concluding remarks.

2. Cable characteristics

The distorting influenc of the cable on the wanted signal is modelled by the transfer function

$$G_{\mathrm{k}}(f) = \mathrm{e}^{-l\sqrt{\mathrm{j}\frac{f}{f_0}}} \ , \qquad (1)$$

where l denotes the cable length (in km) and f_0 represents the characteristic cable frequency (in $\mathrm{MHz}\cdot\mathrm{km}^2$) [14]. Furthermore, the far-end crosstalk coupling is covered by the transfer function $G_{\mathrm{F}}(f)$ with

$$|G_{\mathrm{F}}(f)|^2 = K_{\mathrm{F}} \cdot l \cdot f^2 \ , \qquad (2)$$

whereby K_{F} is a FEXT coupling constant, which depends on the cable properties such as the type of insulation, the number of wire pairs and the kind of combination of the wire pairs within the binders [2], [15], [16]. If the far-end crosstalk from several neighbouring wire pairs is considered, with increasing distance of the disturbing wire pair from the considered pair in a cable the impact of far-end crosstalk decreases. Considering n_{F} FEXT-disturbing wire pairs, in conformity with cable measurements, this behaviour can be modelled by [2]

$$K_{\mathrm{F}} = n_{\mathrm{F}}^{0.6} \cdot K_{\mathrm{F1}} \ , \qquad (3)$$

where K_{F1} is the FEXT coupling constant for one disturbing wire pair. By (3) it is taken into account, that the wire pairs, which are located farther away from the considered wire pair contribute less to the FEXT disturbance than the wire pairs, which are located closer to the considered wire pair [2].

3. MIMO-OFDM System model and quality criteria

Within this contribution a whole cable binder is considered as a transmission channel with multiple inputs and multiple outputs (MIMO). The considered cable binder consists of n wire pairs and therefore a $(n,\ n)$ MIMO transmission system arises. The mapping of the transmit signals $u_{\mathrm{s}\,\mu}(t)$ onto the received signals $u_{\mathrm{k}\,\mu}(t)$ (with $\mu = 1,\ldots,n$) can be described accordingly to Fig. 1. On each wire pair of the cable binder OFDM (orthogonal frequency division multiplexing) is used as transmission technique to combat the effects of the frequency-selective channel [17], [18]. In such a (n,n)-MIMO-OFDM system, an N-point IFFT (N subchannels) modulated data signal is transmitted on every wire pair. The system is modelled by

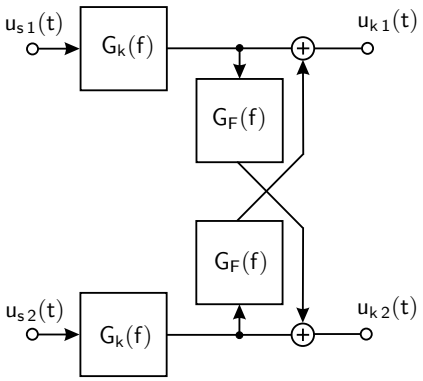

Fig. 1. MIMO cable transmission model system with FEXT ($n = 2$)

$$\mathbf{u} = \mathbf{R}\cdot\mathbf{c} + \mathbf{w} \ . \qquad (4)$$

In (4), $\mathbf{c}$ is the $(L\times 1)$ transmitted signal vector containing the $L = N\,n$ complex input symbols transmitted over all n wire pairs. Using OFDM with a sufficien guard interval length, only symbols that are transmitted over the same subcarrier can interfere each other. The data vector $\mathbf{c}$ can be decomposed according to

$$\mathbf{c} = \left(\mathbf{c}_1^{\mathrm{T}},\ldots,\mathbf{c}_\kappa^{\mathrm{T}},\ldots,\mathbf{c}_N^{\mathrm{T}}\right)^{\mathrm{T}} \ , \qquad (5)$$

where the $(n\times 1)$ vector $\mathbf{c}_\kappa$ contains the complex input symbols transmitted over the κth subcarrier

on each wire pair. Furthermore $\mathbf{u}$ describes the $(L \times 1)$ received vector and $\mathbf{w}$ is the $(L \times 1)$ vector of the Additive, White Gaussian Noise (AWGN) having a variance of U_{R}^2 for both the real and imaginary parts. Applying OFDM with a sufficien guard interval length, the matrix $\mathbf{R}$ in (4) gets a block diagonal structure according to

$$\mathbf{R} = \begin{bmatrix} \mathbf{R}_1 & \mathbf{0} & \cdots & \mathbf{0} \\ \mathbf{0} & \mathbf{R}_2 & \ddots & \vdots \\ \vdots & \ddots & \ddots & \vdots \\ \mathbf{0} & \mathbf{0} & \cdots & \mathbf{R}_N \end{bmatrix} . \tag{6}$$

In (6), zero-matrices are denoted by $\mathbf{0}$ and for the matrices $\mathbf{R}_\kappa$ (with $\kappa = 1, \ldots, N$) the following syntax is used

$$\mathbf{R}_\kappa = \begin{bmatrix} r_{1\,1}^{(\kappa)} & \cdots & r_{1\,n}^{(\kappa)} \\ \vdots & \ddots & \vdots \\ r_{n\,1}^{(\kappa)} & \cdots & r_{n\,n}^{(\kappa)} \end{bmatrix} , \tag{7}$$

with the elements describing the couplings of the data symbols on the subchannel κ as define in [1]. The elements $r_{\nu\,\mu}^{(\kappa)}$ (for $\nu \neq \mu$) are assumed to be identical for each κ, although in practical systems the coupling between the wire pairs is slightly different and it depends on their arrangement in the binder [2]. The subcarrier-specifi interferences introduced by the non-diagonal matrix $\mathbf{R}_\kappa$ require appropriate signal processing strategies. A popular technique is based on the singular value decomposition (SVD) of the matrix $\mathbf{R}_\kappa$, which can be written as $\mathbf{R}_\kappa = \mathbf{S}_\kappa \cdot \mathbf{V}_\kappa \cdot \mathbf{D}_\kappa^{\mathrm{H}}$, where $\mathbf{S}_\kappa$ and $\mathbf{D}_\kappa^{\mathrm{H}}$ are unitary matrices and $\mathbf{V}_\kappa$ is a real-valued diagonal matrix of the positive square roots of the eigenvalues of the matrix $\mathbf{R}_\kappa^{\mathrm{H}}\,\mathbf{R}_\kappa$ sorted in descending order[1]. Using $\mathbf{D}_\kappa$ as preprocessing matrix at the transmitter and $\mathbf{S}_\kappa^{\mathrm{H}}$ as postprocessing matrix at the receiver side, the overall transmission relationship results in

$$\mathbf{y}_\kappa = \mathbf{S}_\kappa^{\mathrm{H}} \left(\mathbf{R}_\kappa \cdot \mathbf{D}_\kappa \cdot \mathbf{c}_\kappa + \mathbf{w}_\kappa \right) = \mathbf{V}_\kappa \cdot \mathbf{c}_\kappa + \tilde{\mathbf{w}}_\kappa . \tag{8}$$

Here, the $(n \times n)$ matrix $\mathbf{R}_\kappa$ is transformed into n independent, non-interfering layers having unequal gains. Taking all N matrices $\mathbf{R}_\kappa$ with (with $\kappa = 1, \ldots, N$) into account, the channel matrix $\mathbf{R}$ is decomposed into $L = N\,n$ independent, non-interfering layers having unequal gains.

In general, the quality of data transmission can be informally assessed by using the signal-to-noise ratio (SNR) at the detector's input define by the half vertical eye opening and the noise power per quadrature component according to

$$\varrho = \frac{(\text{Half vertical eye opening})^2}{\text{Noise Power}} = \frac{(U_{\mathrm{A}})^2}{(U_{\mathrm{R}})^2} , \tag{9}$$

which is often used as a quality parameter [19]. The relationship between the signal-to-noise ratio $\varrho = U_{\mathrm{A}}^2 / U_{\mathrm{R}}^2$ and the bit-error probability evaluated for AWGN channels and M-ary Quadrature Amplitude Modulation (QAM) is given by [20]

$$P_{\mathrm{BER}} = \frac{2}{\log_2(M)} \left(1 - \frac{1}{\sqrt{M}} \right) \operatorname{erfc}\left(\sqrt{\frac{\varrho}{2}} \right) . \tag{10}$$

When applying the proposed system structure, the SVD-based equalization leads to different eye openings per layer ℓ according to

$$U_{\mathrm{A}}^{(\ell)} = \sqrt{\xi_\ell} \cdot U_{\mathrm{s}\,\ell} , \tag{11}$$

where $U_{\mathrm{s}\,\ell}$ denotes the half-level transmit amplitude assuming M_ℓ-ary QAM and $\sqrt{\xi_\ell}$ represents the weighting factor (singular value) resulting from the subcarrier-based equalization. Together with the noise power per quadrature component, the SNR per layer becomes

$$\varrho^{(\ell)} = \frac{\left(U_{\mathrm{A}}^{(\ell)} \right)^2}{U_{\mathrm{R}}^2} = \xi_\ell \, \frac{(U_{\mathrm{s}\,\ell})^2}{U_{\mathrm{R}}^2} . \tag{12}$$

The bit-error probability per layer ℓ is given by [19]

$$P_{\mathrm{BER}}^{(\ell)} = \frac{2\left(1 - \frac{1}{\sqrt{M_\ell}}\right)}{\log_2(M_\ell)} \operatorname{erfc}\left(\sqrt{\frac{\xi_\ell}{2}} \cdot \frac{U_{\mathrm{s}\,\ell}}{U_{\mathrm{R}}} \right) . \tag{13}$$

The resulting average bit-error probability assuming different layer-specifi QAM constellation sizes results in

$$P_{\mathrm{BER}} = \frac{1}{\sum_{\nu=1}^{L} \log_2(M_\nu)} \sum_{\ell=1}^{L} \log_2(M_\ell)\, P_{\mathrm{BER}}^{(\ell)} . \tag{14}$$

Therein the number of transmitted bits per data block results in

$$R = \sum_{\ell=1}^{L} \log_2 M_\ell , \tag{15}$$

assuming that all L layers are used for the data transmission. Considering QAM constellations, the average transmit power $P_{\mathrm{s}\,\ell}$ per layer ℓ may be expressed as [21], [22]

$$P_{\mathrm{s}\,\ell} = \frac{2}{3}\, U_{\mathrm{s}\,\ell}^2 \,(M_\ell - 1) . \tag{16}$$

Combining (12) and (16), the layer-specifi SNR results in

$$\varrho^{(\ell)} = \xi_\ell \, \frac{3}{2\,(M_\ell - 1)} \, \frac{P_{\mathrm{s}\,\ell}}{U_{\mathrm{R}}^2} . \tag{17}$$

[1] The transpose and conjugate transpose (Hermitian) of $\mathbf{D}_\kappa$ are denoted by $\mathbf{D}_\kappa^{\mathrm{T}}$ and $\mathbf{D}_\kappa^{\mathrm{H}}$, respectively.

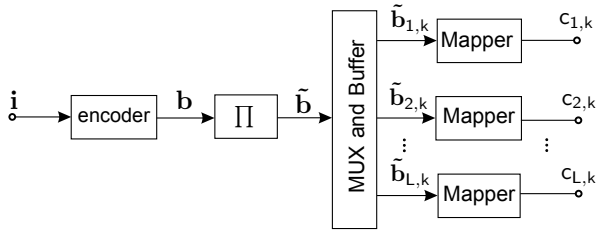

Fig. 2. The channel-encoded MIMO-OFDM transmitter structure

Using a parallel transmission over N subchannels the overall mean transmit power per wire yields to

$$P_{\mathrm{s}} = N \cdot P_{\mathrm{s}\,\ell} = N\,\frac{2}{3}\,U_{\mathrm{s}\,\ell}^2\,(M_\ell - 1)\ , \qquad (18)$$

and results in a total transmit power of $n\,P_{\mathrm{s}}$ by taking n wire-pairs into account. Assuming that the transmit power is uniformly distributed over the number of activated layers, i. e., $P_{\mathrm{s}\,\ell} = P_{\mathrm{s}}/N$, the half-level transmit amplitude $U_{\mathrm{s}\,\ell}$ per layer results in

$$U_{\mathrm{s}\,\ell} = \sqrt{\frac{3\,P_{\mathrm{s}}}{2\,N\,(M_\ell - 1)}}\ . \qquad (19)$$

4. Coded MIMO-OFDM System

The transmitter structure including channel coding is depicted in Fig. 2. The encoder employs a non-recursive, non-systematic convolutional (NSC) code. The uncoded information is organized in blocks of N_{i} bits, consisting of at least 1000 bits, depending on the specifi transmission mode used. Each data block $\mathbf{i}$ is encoded and results in the block $\mathbf{b}$ consisting of N_{b} encoded bits, including a given number of termination bits. The encoded bits are interleaved using a random interleaver and stored in the vector $\tilde{\mathbf{b}}$. The encoded and interleaved bits are then mapped onto the layers. The task of the multiplexer and buffer block of Fig. 2 is to divide the vector of encoded and interleaved information bits $\tilde{\mathbf{b}}$ into subvectors $(\tilde{\mathbf{b}}_{1,k}, \tilde{\mathbf{b}}_{2,k}, \cdots, \tilde{\mathbf{b}}_{L,k})$, each consisting of R bits according to the chosen throughput. The individual binary data vectors $\tilde{\mathbf{b}}_{\ell,k}$ are then mapped to the QAM symbols $c_{\ell,k}$ according to the specifi mapper used [1].

5. Results

The FEXT impact is in particular strong for short cables [2]. Therefore for numerical analysis an exemplary cable of length $l = 0.4\,\mathrm{km}$ with $n = 10$ wire pairs is chosen. The wire diameter is $0.6\,\mathrm{mm}$ and hence a characteristic cable frequency of $f_0 = 0.178\,\mathrm{MHz}\cdot\mathrm{km}^2$ is assumed. On each of the wire pairs a multicarrier system with $N = 10$ subcarriers was considered. The actual crosstalk circumstances are difficul to acquire and they vary from cable to cable. Therefore exemplary mean FEXT coupling constants of $K_{\mathrm{F}} = 10^{-13} \ldots 10^{-15}\,(\mathrm{Hz}^2\cdot\mathrm{km})^{-1}$ are employed [2], [23]. The average transmit power on each wire pair is supposed to be $P_{\mathrm{s}} = 1\,\mathrm{V}^2$ and as an external disturbance a white Gaussian noise with power spectral density Ψ_0 is assumed. Identical systems on all wire pairs are presumed (multicarrier symbol duration $T_{\mathrm{s}} = 2\,\mu\mathrm{s}$, M-ary QAM and a guard interval length of $T_{\mathrm{g}} = T_{\mathrm{s}}/2$). Furthermore, the baseband channel of the multicarrier system is excluded from the transmission in order to support a parallel analogue telephone service. For a fair comparison the ratio of symbol energy to noise power spectral density at the cable output is define for the MIMO case $(n > 1)$ according to

$$\frac{E_{\mathrm{s}}}{\Psi_0} = (T_{\mathrm{s}} + T_{\mathrm{g}})\ \frac{P_{\mathrm{k}} + (n-1)P_{\mathrm{k\,fn}}}{\Psi_0}\ , \qquad (20)$$

with P_{k} as mean power of the signal on the direct paths at the cable output and $P_{\mathrm{k\,fn}}$ as mean FEXT signal power at the cable output [19].

Using the half-rate, constraint-length $K = 3$ NSC code with the generator polynomials of $(7, 5)$ in octal notation, the performance is analyzed for an effective user throughput of 2 bit/s/Hz. Our results, obtained by analyzing the soft-demapper characteristic (Fig. 3) suggest that the performance of the MIMO-OFDM system is strongly effected by the FEXT coupling. Here it turns out that a heavy FEXT coupling is highly beneficia for a fast convergence as it is can be seen in Fig. 4.

A mapping scheme optimized for perfect *a priori* information has usually a poor performance, when there is no *a priori* information. However, when applying iterative demapping and decoding, large gains can be achieved as long as the reliability of the *a priori* information increases upon increasing the number of iterations. The achievable performance of the iterative decoder is substantially affected by the specifi mapping of the bits to both the QAM symbols as well as to the layers. The influenc of different mapping schemes can be quantifie with the aid of the corresponding Mutual Information between the transmitted M-QAM symbol $c^{(\nu)}$ taken from the signal constellation $\mathcal{C}$ and the received AWGN-contaminated channel output

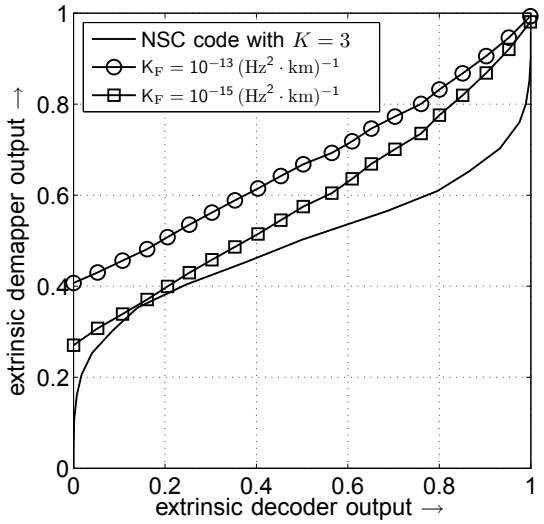

Fig. 3. Exit chart with 16-QAM anti-Gray mapping on all activated layers and the half-rate, constraints length $K = 3$ NSC code with the generator polynomials of $(7, 5)$ in octal notation at $10\,\log_{10}(E_s/\Psi_0) = 20$ dB

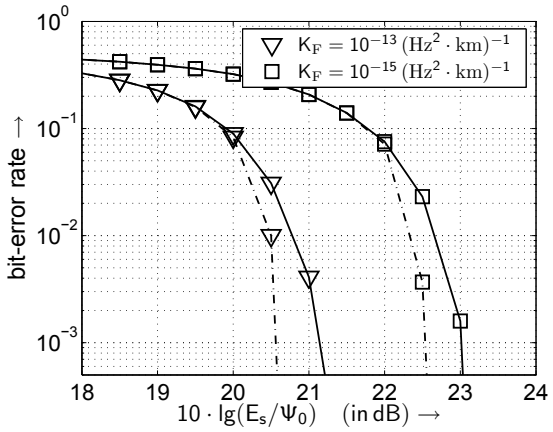

Fig. 4. BER of the iteratively detected channel-encoded MIMO-OFDM system with 16-QAM anti-Gray mapping on all layers (solid line $\triangleq 3$ iterations, dashed line $\triangleq 10$ iterations) using the half-rate, constraint-length $K = 3$ NSC code with the generator polynomials of $(7, 5)$ in octal notation

y, which is given by

$$I(c;y) = \frac{1}{M}\sum_{\nu=1}^{M}\int_{-\infty}^{\infty} p(y|c=c^{(\nu)})\log_2\frac{p(y|c=c^{(\nu)})}{p(y)}\mathrm{d}y \ , \tag{21}$$

assuming that all QAM symbols are equiprobable. The conditional Probability Density Function (PDF) $p(y|c = c^{(\nu)})$ is define as follows

$$p(y|c=c^{(\nu)}) = \frac{1}{2\,\pi\,U_R^2}\exp\left(-\frac{|y-c^{(\nu)}|^2}{2\,U_R^2}\right) \ , \tag{22}$$

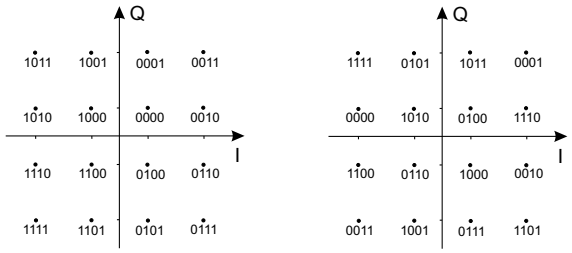

Fig. 5. 16-QAM mapping schemes (left: Gray-coding, right: anti-Gray coding)

with

$$p(y) = \frac{1}{M}\sum_{\nu=1}^{M} p(y|c=c^{(\nu)}) \ . \tag{23}$$

Applying the chain rule, namely that the mutual information between the M-QAM symbol $c^{(\nu)} \in \mathcal{C}$, consisting of the m-bit vector $(\tilde{b}^{(1)}, \cdots, \tilde{b}^{(m)})$, and the received AWGN-contaminated channel output y can be decomposed into a sum of $m = \log_2(M)$ bitwise mutual information terms I_l, provided l out of that m bits are already known to the receiver, leads to

$$I(c;y) = I(\tilde{b}^{(1)}, \cdots, \tilde{b}^{(m)}; y) = \sum_{\ell=0}^{m-1} I_\ell \ . \tag{24}$$

Therein, I_ℓ represents the average of the mutual information, which was averaged over all bits of the mapping. While the employment of the classic Gray-mapping is appropriate in the absence of *a priori* information, the availability of *a priori* information in iteratively detected schemes requires an exhaustive search for findin the best non-Gray – synonymously also referred to as anti-Gray – mapping scheme [24], [25]. Investigations in [26] have shown that the maximum iteration gain can only be guaranteed, if anti-Gray mapping is used on all activated layers. As an example,

TABLE I

CONDITIONAL MUTUAL INFORMATION FOR DIFFERENT 16-QAM MAPPING SCHEMES INTRODUCED IN FIG. 5

	I_0	I_1	I_2	I_3	$I(c;y)$
Gray	0.2117	0.2118	0.2118	0.2118	0.8471
anti-Gray	0.0792	0.1634	0.2768	0.3276	0.8471

Tab. I shows the conditional mutual information at an exemplarily considered noise power per quadrature component of $U_R^2 = 0.05$ for the two 16-QAM mapping schemes shown in Fig. 5, which have been used in assisted iteratively detected bit-interleaved coded modulation schemes [24].

Our BER curves obtained by computer simulations show that the FEXT coupling between neighbouring wire pairs seems to be a real catalyst for the overall performance that is effected by both the cable length as well as the cable properties such as the type of isolation, the number of wire pairs and the kind of combination of the wire pairs within the binders.

6. Conclusion

In this contribution the FEXT impact in iteratively detected MIMO-OFDM transmission schemes has been studied. Our results show that FEXT is not necessarily a limiting factor if appropriate signal processing strategies are used. Our results show that a heavy FEXT impact is overall beneficia for a good convergence behaviour at low SNR.

ACKNOWLEDGEMENT

The authors wish to thank the anonymous reviewers for hints and comments that helped to improve the paper and for bringing [13] and [27] to their attention.

References

[1] A. Ahrens and C. Lange, “Iteratively Detected MIMO-OFDM Twisted-Pair Transmission Schemes,” in *E-business and Telecommunications*, ser. Communications in Computer and Information Science, J. Filipe and M. S. Obaidat, Eds. Heidelberg: Springer, 2008.

[2] C. Valenti, “NEXT and FEXT Models for Twisted-Pair North American Loop Plant,” *IEEE Journal on Selected Areas in Communications*, vol. 20, no. 5, pp. 893–900, June 2002.

[3] W. van Etten, “An Optimum Linear Receiver for Multiple Channel Digital Transmission Systems,” *IEEE Transactions on Communications*, vol. 23, no. 8, pp. 828–834, 1975.

[4] C. Lange and A. Ahrens, “Channel capacity of twisted wire pairs in multi-pair symmetric copper cables.” in *Fifth International Conference on Information, Communications and Signal Processing (ICICS)*, Bangkok (Thailand), 06.–09. Dezember 2005, pp. 1062–1066.

[5] G. G. Raleigh and J. M. Cioffi “Spatio-Temporal Coding for Wireless Communication.” *IEEE Transactions on Communications*, vol. 46, no. 3, pp. 357–366, March 1998.

[6] G. G. Raleigh and V. K. Jones, “Multivariate Modulation and Coding for Wireless Communication.” *IEEE Journal on Selected Areas in Communications*, vol. 17, no. 5, pp. 851–866, May 1999.

[7] M. L. Honig, K. Steiglitz, and B. Gopinath, “Multichannel Signal Processing for Data Communications in the Presence of Crosstalk,” *IEEE Transactions on Communications*, vol. 38, no. 4, pp. 551–558, April 1990.

[8] C. Lange and A. Ahrens, “Effect of Far-End Crosstalk in Multi-Pair Symmetric Copper Cables.” in *XXI Krajowe Sympozjum Telekomunikacji (KST)*, Bydgoszcz (Poland), 07.–09. September 2005, pp. 181–190.

[9] G. Caire, G. Taricco, and E. Biglieri, “Bit-Interleaved Coded Modulation,” *IEEE Transactions on Information Theory*, vol. 44, no. 3, pp. 927–946, March 1998.

[10] L. R. Bahl, J. Cocke, F. Jelinek, and J. Raviv, “Optimal Decoding of Linear Codes for Minimizing Symbol Error Rate,” *IEEE Transactions on Information Theory*, vol. 20, no. 3, pp. 284–287, March 1974.

[11] R. Cendrillon, G. Ginis, M. Moonen, J. Verlinden, and B. T., “Improved Linear Crosstalk Precompensation for DSL,” in *IEEE International Conference on Acoustics, Speech and Signal Processing (ICASSP)*, September 2004.

[12] R. F. H. Fischer, *Precoding and Signal Shaping for Digital Transmission*. New York: John Wiley, 2002.

[13] R. Cendrillon, G. Ginis, E. Van den Bogaert, and M. Moonen, “A Near-Optimal Linear Crosstalk Canceler for Upstream VDSL,” *IEEE Transactions on Signal Processing*, vol. 54, no. 8, pp. 3136 – 3146, 2006.

[14] D. Kreß and M. Krieghoff, “Elementare Approximation und Entzerrung bei der Übertragung von PCM-Signalen über Koaxialkabel,” *Nachrichtentechnik Elektronik*, vol. 23, no. 6, pp. 225–227, 1973.

[15] S. Galli and K. J. Kerpez, “Methods of Summing Crosstalk From Mixed Sources—Part I: Theoretical Analysis,” *IEEE Transactions on Communications*, vol. 50, no. 3, pp. 453–461, März 2002.

[16] ——, “Methods of Summing Crosstalk From Mixed Sources—Part II: Performance Results,” *IEEE Transactions on Communications*, vol. 50, no. 4, pp. 600–607, April 2002.

[17] A. R. S. Bahai and B. R. Saltzberg, *Multi-Carrier Digital Communications – Theory and Applications of OFDM*. New York, Boston, Dordrecht, London, Moskau: Kluwer Academic/Plenum Publishers, 1999.

[18] J. A. C. Bingham, *ADSL, VDSL, and Multicarrier Modulation*. New York: Wiley, 2000.

[19] A. Ahrens and C. Lange, “Optimal Power Allocation in a MIMO-OFDM Twisted Pair Transmission System with Far-End Crosstalk.” in *International Conference on Signal Processing and Multimedia Applications (SIGMAP)*, Setúbal (Portugal), 07.–10. August 2006.

[20] I. Kalet, “Optimization of Linearly Equalized QAM,” *IEEE Transactions on Communications*, vol. 35, no. 11, pp. 1234–1236, November 1987.

[21] G. D. Forney, R. G. Gallager, G. R. Lang, F. M. Longstaff, and S. U. Qureshi, “Efficien Modulation for Band-Limited Channels,” *IEEE Journal on Selected Areas in Communications*, vol. 2, no. 5, pp. 632–647, 1984.

[22] I. Kalet, “The Multitone Channel.” *IEEE Transactions on Communications*, vol. 37, no. 2, pp. 119–124, Februar 1989.

[23] J. T. Aslanis and J. M. Cioffi “Achievable Information Rates on Digital Subscriber Loops: Limiting Information Rates with Crosstalk Noise,” *IEEE Transactions on Communications*, vol. 40, no. 2, pp. 361–372, February 1992.

[24] J. A. Chindapol, A. Ritcey, “Design, Analysis, and Performance Evaluation for BICM-ID withsquare QAM Constellations in Rayleigh Fading Channels,” *IEEE Journal on Selected Areas in Communications*, vol. 19, no. 5, pp. 944–957, May 2001.

[25] A. Sezgin, D. Wübben, R. Böhnke, and V. Kühn, “On EXIT-Charts for Space-Time Block Codes.” in *IEEE International Symposium on Information Theory (ISIT)*, Yokohama, Japan, 29. June - 4. July 2003.

[26] A. Ahrens and V. Kühn, “Analysis of SVD-Aided, Iteratively Detected Spatial Division Multiplexing using EXIT Charts.” in *12th International OFDM-Workshop*, Hamburg, 29.–30. August 2007, pp. 271–275.

[27] G. Ginis and J. M. Cioffi “Vectored Transmission for Digital Subscriber Line Systems,” *IEEE Journal on Selected Areas in Communications*, vol. 20, no. 5, pp. 1085–1104, 2002.